nature medicine

Alum interaction with dendritic cell membrane lipids is essential for its adjuvanticity

Tracy L Flach[1,7], Gilbert Ng[1,7], Aswin Hari[1], Melanie D Desrosiers[1], Ping Zhang[2], Sandra M Ward[2], Mark E Seamone[3], Akosua Vilaysane[3], Ashley D Mucsi[1], Yin Fong[1], Elmar Prenner[4], Chang Chun Ling[2], Jurg Tschopp[5], Daniel A Muruve[3], Matthias W Amrein[6] & Yan Shi[1]

As an approved vaccine adjuvant for use in humans, alum has vast health implications, but, as it is a crystal, questions remain regarding its mechanism. Furthermore, little is known about the target cells, receptors, and signaling pathways engaged by alum. Here we report that, independent of inflammasome and membrane proteins, alum binds dendritic cell (DC) plasma membrane lipids with substantial force. Subsequent lipid sorting activates an abortive phagocytic response that leads to antigen uptake. Such activated DCs, without further association with alum, show high affinity and stable binding with CD4$^+$ T cells via the adhesion molecules intercellular adhesion molecule-1 (ICAM-1) and lymphocyte function–associated antigen-1 (LFA-1). We propose that alum triggers DC responses by altering membrane lipid structures. This study therefore suggests an unexpected mechanism for how this crystalline structure interacts with the immune system and how the DC plasma membrane may behave as a general sensor for solid structures.

Alum, loosely defined as any trivalent aluminum-containing salt, was first tested as an adjuvant by A.T. Glenny in a tetanus toxin vaccine[1]. Subsequently, alum was vital to the success of Jonas Salk's polio virus vaccine in the 1950s[2]. It has become the standard adjuvant for humans, used in the great majority of immunization regimens. Various hypotheses regarding alum's mechanism of action have been proposed[3].

It was first thought that antigens mixed with alum might have a prolonged presence in tissues. However, this 'depot effect' has been discarded[4]. Alum injection sites can be excised without affecting alum's adjuvancity[3]. It has been shown that alum vaccination led to an increase in interleukin-4 (IL-4)–producing cells that bear the monocyte and neutrophil marker Gr1[5]. However, it was not clear if these cells were the initial responders to alum. It was found that alum triggered adjuvanticity by inducing uric acid release[6]. However, injection of alum triggers mild tissue irritation, suggesting little cell death or uric acid release. It has been reported that alum relies on the NACHT, LRR and PYD domains–containing protein-3 (Nlrp3) inflammasome for its adjuvanticity[7,8]. The engulfed particles trigger lysosomal membrane damage, leading to Nlrp3 activation via cathepsin B[9]. This mechanism has been disputed by other reports[10–12].

There are several fundamental questions remaining (also see ref. 3). First, what cells initially sense this crystal? Second, is there an alum-specific receptor on the cell membrane? Third, why does alum only enhance humoral responses? Last, what is the role of inflammasomes in alum's adjuvanticity?

We report here that alum does not have a receptor on the DC surface. It directly engages lipids in the plasma membrane of DCs, leading to lipid sorting similar to monosodium urate (MSU) crystals that involves the aggregation of immunoreceptor signaling motif (ITAM)-containing receptors, and subsequent spleen tyrosine kinase (Syk)- and phosphoinositide 3-kinase (PI3K)-mediated phagocytic responses. Alum does not enter the cell; it instead delivers the admixed soluble antigen across the plasma membrane. DCs thus engaged by alum develop a strong affinity for CD4$^+$ T cells. We provide evidence that this strong binding is mediated by ICAM-1 and LFA-1. These observed activation events are intact in the absence of inflammasome activation. We feel that our study will have an impact in future vaccine design and on general views of how tissues handle solid structures without protein-based receptors.

RESULTS

Alum crystals induce abortive phagocytosis

Using atomic force microscopy (AFM)[13], we first observed lipid-based interactions for MSU[14]. Lipid sorting leads to the aggregation of ITAM-containing receptors and Syk recruitment, resulting in a PI3K-mediated inflammatory phagocytic response. Although alum compositions vary, the admixing of antigen with alum requires a step of crystal rederivatization[15,16]. Alum crystal surfaces are different from MSU crystals (**Supplementary Fig. 1**). Most alum preparations are not suitable for AFM operations, because their surfaces are too weak for gluing or they dissolve rapidly in solution. Cesium alum (CsAl), rederivatized

[1]Immunology Research Group, Department of Microbiology & Infectious Diseases, and Snyder Institute, University of Calgary, Calgary, Alberta, Canada. [2]Department of Chemistry and Alberta Ingenuity Center for Carbohydrate Science, University of Calgary, Calgary, Alberta, Canada. [3]Department of Medicine, University of Calgary, Calgary, Alberta, Canada. [4]Department of Biological Sciences, University of Calgary, Calgary, Alberta, Canada. [5]Department of Biochemistry, University of Lausanne, Epalinges, Switzerland. [6]Department of Biology and Anatomy, University of Calgary, Calgary, Alberta, Canada. [7]These authors contributed equally to this work. Correspondence should be addressed to Y.S. (yshi@ucalgary.ca).

Received 26 July 2010; accepted 18 January 2011; published online 13 March 2011; doi:10.1038/nm.2306

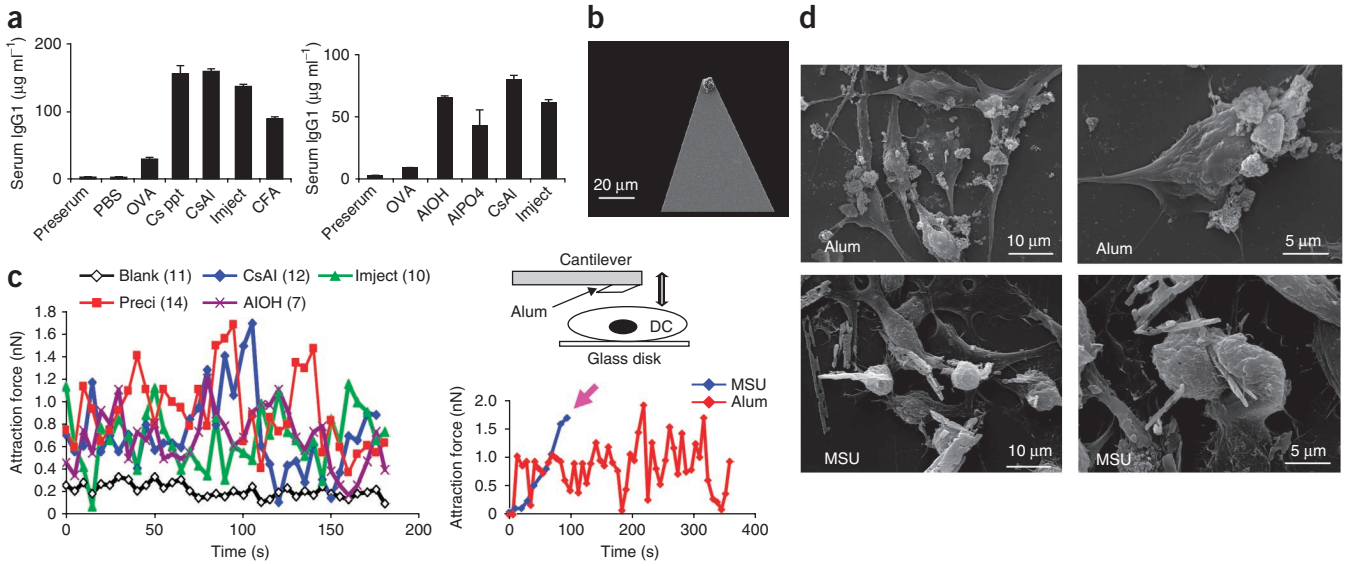

Figure 1 Alum shows affinity for DC surface without inducing phagocytosis. (**a**) Left, serum IgG1 OVA-specific antibody titers 2 weeks after immunization with the indicated type of alum as adjuvant. Right, similar to the left except that clinical alum AlOH and AlPO4 were tested. (**b**) An SEM image of CsAl mounted on an AFM tip with epoxy. (**c**) Typical binding forces between a DC2.4 cell and four forms of alum. Blank refers to a tip with no alum attached. The number in parentheses indicates number of independent repeats of that operation (a representative curve for each is shown). At top right is a schematic depiction of the assay. The bottom right graph is a comparison of force curves between an MSU tip and an alum tip in their interaction with a DC2.4 cell. DC2.4 cell interaction with an MSU (or latex, not shown) tip is characterized by a gradual increase in binding strength and by a point of loss of retraction force curve indicated by the arrow (point of irreversible binding: phagocytosis). (**d**) SEM of DC2.4 cells cultured for 2 h with either CsAl (top) or MSU (bottom).

CsAl crystal, Imject (a commercial preparation containing aluminum and magnesium hydroxide) and AlOH (a preparation used in human vaccines) can be mounted onto AFM tips (**Supplementary Fig. 1**). All these types of experimental alum enhanced ovalbumin (OVA)-specific antibody titers in mice after OVA challenge similar to clinical regimens of AlOH and $AlPO_4$ (**Fig. 1a**) (see Online Methods). Using epoxy, we glued individual ~5-μm–sized alum crystals to tipless silicone AFM cantilevers (**Fig. 1b**). A custom-built humidified AFM enclosure that permits long term operation under 5% CO_2 and 37 °C was installed. The cantilevers were lowered to make contact with individual DC2.4 cells (DC cell line)[14]. All alum preparations generated binding affinity to DCs (**Fig. 1c**; statistical analyses are in the **Supplementary Data**). AlOH tips also showed the oscillating high-to-low binding pattern (**Fig. 1c**). Unexpectedly, unlike tips with MSU and latex beads, alum tips did not produce irreversible phagocytosis characterized by inseparable binding[14]; instead, the DCs remained responsive to the approaching alum tips with oscillating binding forces (**Fig. 1c**). We observed that alum crystals glued to the AFM cantilever became progressively smaller after multiple cell contacts. Possibly, some layers of the crystal were 'peeled off' by the approaching plasma membrane. This lack of phagocytosis of alum was corroborated by electron microscopy analysis demonstrating the immediate engulfment and internalization of MSU crystals by DCs, an event that did not occur with alum, even after long-term incubation (**Fig. 1d**). In the few cases where internalized alum was visible, cells showed extensive signs of membrane damage (**Supplementary Fig. 2**).

DCs are the only target cells for alum

To search for cell types that interact with alum, we measured the binding of an alum tip to macrophage, DC and B cell lines. B cells were cultured on poly–D-lysine–coated disks for firm attachment. In this assay, DCs (DC2.4 and phorbol-12-myristate-13-acetate (PMA)-induced THP-1 cells) were the only cell type that produced a substantial binding force (**Fig. 2a**). Similarly, using primary mouse bone marrow–derived DCs or macrophages (produced by stimulation with granulocyte-macrophage colony–stimulating factor (GM-CSF) and IL-4 or DAP cell culture supernatant, respectively) or splenic B cells (isolated with magnetic cell sorting beads, see Online Methods), only DCs showed a binding force with an alum tip (**Fig. 2b**). AlOH showed identical binding to DC2.4 (data not shown). Such forces were absent with RAW 264.7 cells (**Supplementary Fig. 3**). These results suggest that DCs may serve as the first point of contact for alum. As DCs treated with alum cannot finish phagocytosis, we investigated whether very fine alum particles or resolubilized alum entered DCs. We incubated DC2.4 cells with alum for 2 h, washed them and analyzed them by scanning electron microscopy (SEM). In addition to obtaining images (**Fig. 2c**), we performed energy-dispersive X-ray spectroscopy microanalysis (EDS), which registers the elemental composition of targets[17]. The SEM electron bombing characteristic of each element is based upon the principle of electron quantum shift. As aluminum is a rare element in biological systems[18], we used carbon (enriched in cells compared with glass background) as the base reading and aluminum / carbon ratios to analyze the distribution. The result showed no signal of aluminum inside DCs compared with the natural contamination in the glass slide (**Fig. 2c**). Therefore, alum interacts with but seldom enters DCs *in vitro*, probably owing to the incomplete phagocytosis.

Our previous work has also shown that this type of affinity binding is intact after myeloid differentiation factor-88 and TIR-domain-containing adapter-inducing interferon-β protein double knockout[14]. Here we performed the assay with Toll-like receptor 4 (TLR4)-knockout DCs and observed the same outcome (**Fig. 2d**). In addition, we tested whether lipopolysaccharide (LPS)-treated DCs (DC2.4) show affinity for all solid structures, such as a tip. We treated DC2.4 cells with LPS for a short period and measured the binding to

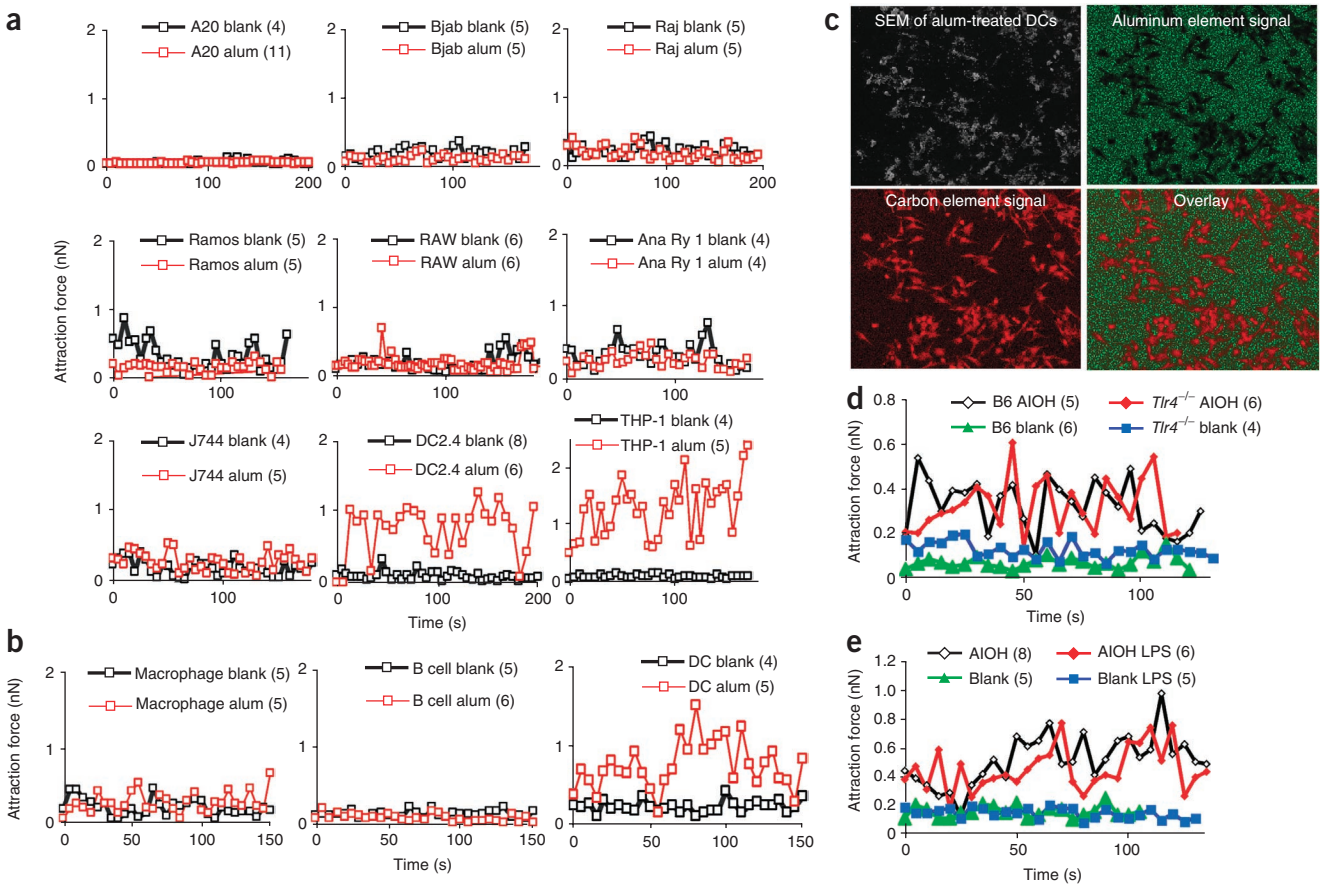

Figure 2 Alum targets only DCs. (**a**) The binding forces of the indicated cells with a CsAl tip as compared to a blank tip. B cells (A20, Bjab, Raj and Ramos), macrophages (RAW 264.7, Ana Ry 1 and J744) and DCs (DC2.4 and PMA-transformed THP-1) were cultured on glass disks by direct adhesion or via a poly-D-lysine substrate coating. (**b**) Similar to **a** except that GM-CSF plus IL-4 and DAP supernatant were used to differentiate BMDCs and macrophages, respectively, and magnetic cell sorting beads were used to purify splenic B cells. All examined with an Imject tip. (**c**) Environmental SEM image and EDS analysis of alum (CsAl precipitate) content in DC2.4 cells treated with alum for 2 h. Cells were washed three times without further treatment or gold sputter coating before data collection. In areas of high carbon reading, the aluminum (natural contaminant) in the glass is shielded from the electron beams due to the cell mass. (**d**) Similar to **b** except that BMDCs from C57BL/6 or TLR4-knockout mice were contacted by AlOH. (**e**) Similar to **b** except that DC2.4 cells were pretreated with 10 μg ml^{-1} of LPS for 30 min before the assay.

a cantilever. The forces remained at the background (**Fig. 2e**). These results suggest that LPS contamination is not involved.

Alum requires multiple lipids for sustained membrane binding

To test whether lipids were responsible for the attachment of alum to DCs, we first wanted to exclude any role of external cell surface proteins. DC2.4 cells were treated with pronase and trapped in a nickel grid[14]. These cells showed normal binding intensity with alum (**Supplementary Fig. 4**), suggesting a lipid-based binding mechanism. Next, we stained alum crystals with fluorescently labeled phosphatidylcholine, phosphatidylethanolamine, sphingomyelin and cholesterol. Alum was stained strongly by sphingomyelin and cholesterol and with intermediate staining by phosphatidylcholine and phosphatidylethanolamine (**Fig. 3a**). To prove the concept of direct lipid engagement, we determined alum affinity with a self-assembled monolayer of synthetic cholesterol (with an aliphatic chain extension) attached to a gold-coated AFM tip through a thiol-gold bond. Alum bound cholesterol in its biological orientation with higher affinity (**Fig. 3b**) compared to an inverted control. Furthermore, a similar synthesis of sphingomyelin with an aliphatic extension on its hydrophobic tail was also attached to a gold tip. In this direct comparison, it seemed that sphingomyelin anchored to the tip had a stronger affinity to the alum surface than cholesterol, although both were statistically higher than the blank-tip control (**Fig. 3b**).

Because similar aliphatic chain extensions of phosphatidylcholine and phosphatidylethanolamine are chemically infeasible, we produced bilayer membranes with defined lipid compositions (phosphatidylcholine + phosphatidylethanolamine, phosphatidylcholine + phosphatidylethanolamine + sphingomyelin, phosphatidylcholine + phosphatidylethanolamine + cholesterol, and all four lipids). Bilayers made from phosphatidylcholine and phosphatidylethanolamine showed little interaction with alum. Addition of cholesterol or sphingomyelin produced stronger interactions but the high forces were not observed in all experiments (negative results shown) (**Fig. 3c**). Membranes generated with all four lipids resulted in force curves that were higher, consistent and reproducible (**Fig. 3c**). Unlike the strong interaction between MSU and cholesterol[14], sphingomyelin seemed to be the strongest interaction partner with the alum surface.

Alum triggers lipid sorting on DCs that activates Syk and PI3K

Receptor-independent cell activation is a rapid event originating from lipid sorting[14]. Alum-mediated DC contact was dependent on cholesterol and cellular motility, as both methyl-β-cyclodextrin (MBCD) and cytochalasin B blocked the binding (**Fig. 4a**). AlOH showed an

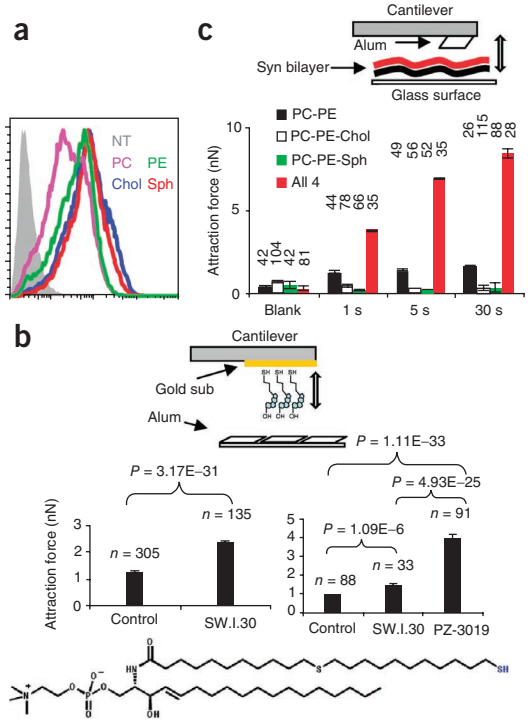

Figure 3 Alum's direct affinity for membrane lipids. (**a**) CsAl precipitate crystals were stained with equal molar concentrations of either phosphatidylcholine (PC), nitro-2-1,3-benzoxadiazol-4-yl (NBD), phosphatidylethanolamine (PE, NBD), sphingomyelin (Sph, BODIPY), or cholesterol (Chol, BODIPY). The bound fluorescence intensity was analyzed by FACS. (**b**) A synthetic cholesterol, SW.I.30, was attached to a gold-coated AFM tip via the thiol group at the end of the aliphatic chain extension. Top, a schematic depiction of the experiments. Left graph, the reading of the maximal attraction forces for SW.I.30. *n* represents the number of independent repeats. Control is a similar synthesis with the aliphatic extension from the hydroxyl group on the head of cholesterol. Right graph, a direct comparison between both cholesterol (SW.I.30) and synthetic sphingomyelin (PZ-3019) in their biological orientation in the membrane with reference to alum crystal contact. Blank, an unmodified tip. PZ-3019 is depicted at the bottom. (**c**) Synthetic bilayer membranes from defined membrane lipids were laid on a glass surface for contact by an Imject tip. The red indicates the upper leaflet for contact. Average binding forces were recorded; the number on the top indicates the number of repeats. Error bars are s.e.m.

identical behavior (**Fig. 4a**). We next examined whether ITAM-containing receptors (segregated into cholesterol-rich domains) were required for the binding between DCs and alum and found that DNAX-activating protein of molecular mass 12 kDa (DAP12) and Fc receptor γ chain double-knockout[19] DCs produced negligible binding with the alum tip (**Fig. 4b**). Similarly, a Syk inhibitor, piceatannol, reduced the binding forces between alum and DCs (**Fig. 4a**). Syk-knockout bone marrow–derived cells (BMDCs) also produced negligible binding (**Fig. 4b**)[20]. The phosphorylation of ITAMs required for Syk recruitment is dependent on Src family tyrosine kinases. DCs deficient in the Src kinases Hck, Fgr and Lyn also showed no binding to the alum tip[21] (**Fig. 4b**). Lastly, wortmannin also inhibited the binding forces, confirming the involvement of PI3K (**Fig. 4a**). Except for the inability of the DCs to complete alum phagocytosis, during the initial contact alum crystals interacted with DCs in a manner similar to other solid structures that involve lipid sorting.

Macrophages are regarded as being similar to DCs in their ability to detect particulate structures. The inability of macrophages to

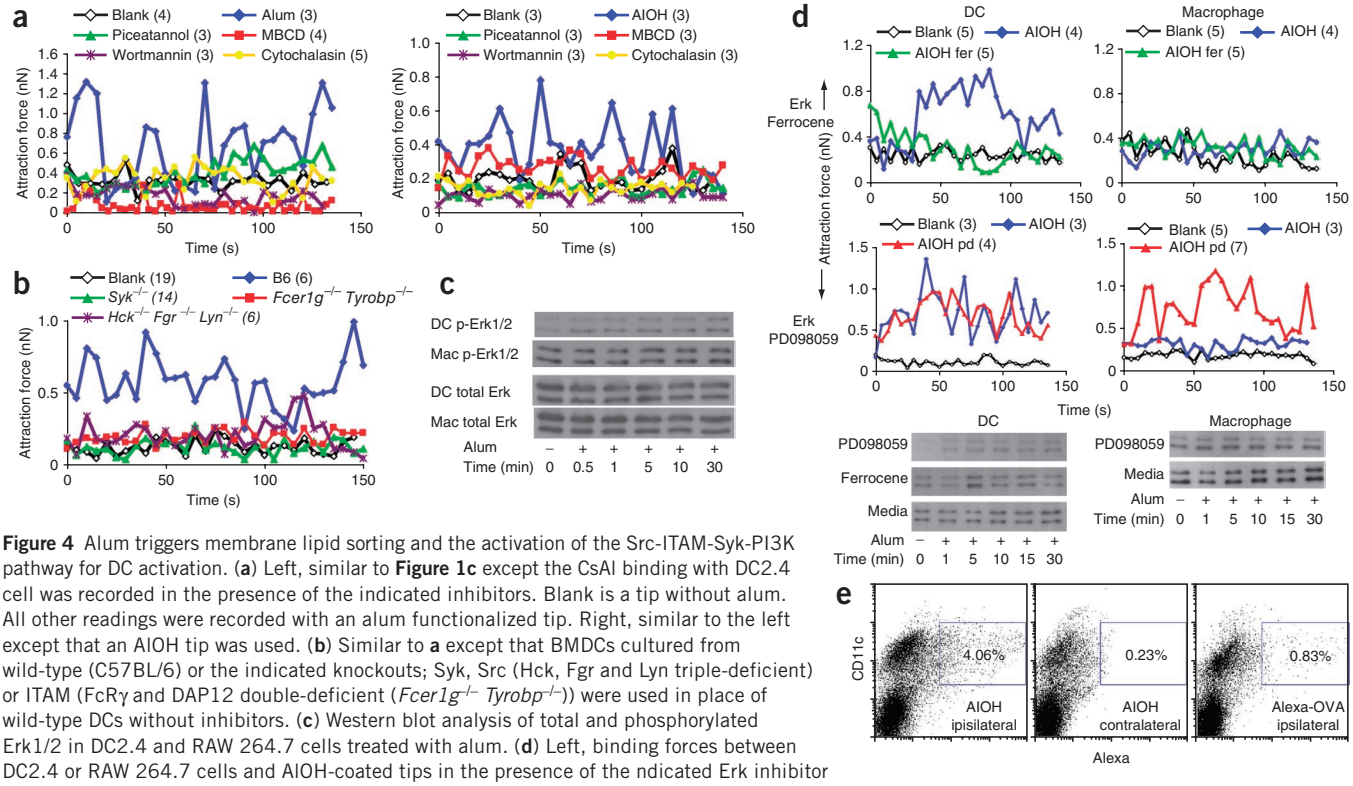

Figure 4 Alum triggers membrane lipid sorting and the activation of the Src-ITAM-Syk-PI3K pathway for DC activation. (**a**) Left, similar to **Figure 1c** except the CsAl binding with DC2.4 cell was recorded in the presence of the indicated inhibitors. Blank is a tip without alum. All other readings were recorded with an alum functionalized tip. Right, similar to the left except that an AlOH tip was used. (**b**) Similar to **a** except that BMDCs cultured from wild-type (C57BL/6) or the indicated knockouts; Syk, Src (Hck, Fgr and Lyn triple-deficient) or ITAM (FcRγ and DAP12 double-deficient (*Fcer1g*$^{-/-}$ *Tyrobp*$^{-/-}$)) were used in place of wild-type DCs without inhibitors. (**c**) Western blot analysis of total and phosphorylated Erk1/2 in DC2.4 and RAW 264.7 cells treated with alum. (**d**) Left, binding forces between DC2.4 or RAW 264.7 cells and AlOH-coated tips in the presence of the ndicated Erk inhibitor or activator. Right, similar to **c** except DC2.4 and RAW 264.7 cells were pretreated with ferrocene and PD098059 before alum stimulation. (**e**) The draining LN CD11c$^+$ cells were analyzed for Alexa levels 36 h after subcutaneous injection of Alexa-OVA and alum mixture as described in the Online Methods. The numbers indicate the CD11c$^+$Alexa$^+$ cells as a percentage of the total cells.

sense alum may be due to a number of reasons. For instance, the lipid compositions of DC and macrophage membranes are different, and they bind to alum and MSU surfaces with different affinities (**Supplementary Fig. 5a**,**b**). We also analyzed their kinase activities. We studied the activation of extracellular signal–regulated kinases 1 and 2 (Erk1/2) in response to alum, as Erk can be triggered by Syk[22]. As expected, Erk1/2 on DCs were phosphorylated at around 5 to 10 min (**Fig. 4c**) after alum contact (**Fig. 4a**,**b**). Erk activation on macrophages was either constant or seen at the earliest possible sample collection point (30 s) after stimulation (**Fig. 4c**). The Erk and PI3K pathways are mutually disruptive; activation of Erk down-regulates PI3K[23,24]. During macrophage activation in response to physical pressure, Erk must be inhibited to allow phagocytosis[25]. An extrapolation is that the higher Erk activity in alum-exposed macrophages blocks PI3K activation, essentially turning down phagocytosis. Such a scenario makes the following prediction: if Erk is activated, DCs will not sense alum; if Erk is blocked on macrophages, they should react to alum as DCs do. We treated DCs and macrophages with an Erk activator (ferrocene) and Erk inhibitors (PD098059 and UO126)[26–28] and confirmed the effect by western blotting (**Fig. 4d**). DCs treated with ferrocene showed minimal binding forces to alum (**Fig. 4d**). PD098059-treated macrophages gained the ability to engage alum, similarly to DCs (**Fig. 4d**). We obtained similar data with UO126 (**Supplementary Fig. 6**). This suggests that DCs and macrophages are different in their responses to alum because of their distinct Erk regulation.

Activation of DCs in the periphery initiates their migration to draining lymph nodes. To see the effect of alum, we mixed Alexa-conjugated OVA with AlOH and subcutaneously injected the mixture or Alexa-OVA alone into the hind flank of C57BL/6 mice. After 36 h, cell suspensions of the draining poplineal lymph nodes were stained for CD11c, and the positive cells were analyzed. Lymph nodes from alum-treated mice had about fourfold more Alexa-positive DCs, suggesting alum increases DC migration (**Fig. 4e**).

Alum adjuvanticity is intact in the absence of inflammasomes

Inflammasomes have been shown to be involved in solid-structure recognition[9,29,30]. However, inflammasome activation is a delayed response[7,30] and requires crystal internalization downstream of membrane-proximal events[31,32]. We produced BMDCs from Nlrp3-knockout and apoptosis-associated speck-like protein (ASC, encoded by *Pycard*)-knockout mice. DCs from both mouse strains produced force curves similar to wild-type controls (**Fig. 5a**), suggesting that the inflammasome is not involved at this step. We then studied cytokine production and DC activation by alum. Consistent with a previous report[33], AlOH did not induce cytokines (**Supplementary Fig. 7a**) or activation marker CD86 expression (**Supplementary Fig. 7b**), in contrast with CsAl. However, upon closer examination, AlOH in Petri dishes showed marked buoyancy and tended to aggregate, whereas CsAl preparations were settled and well dispersed (data not shown). It is possible that cytokine production requires sustained contact, a likely scenario *in vivo*. We therefore carried out assays with CsAl. As expected, IL-1β production was absent in both *Nlrp3*$^{-/-}$ and *Pycard*$^{-/-}$ DCs in response to alum (**Fig. 5**), whereas the expression of tumor necrosis factor-α (TNF-α) and the co-stimulatory molecules CD80, CD86 and CD40 were comparable to wild-type DCs (**Fig. 5b**,**c**). These results suggest that membrane events independent of the Nlrp3 inflammasome are sufficient to mediate DC activation in response to alum. As expected, similar assays performed in Syk-knockout, FcRγ– and DAP12–double-knockout and Hck–, Fgr– and Lyn–triple-knockout cells showed reduced cytokine production in response to alum (**Fig. 5d**), further suggesting an essential role for lipid sorting in DC activation. We performed binding assays of *Nlrp3*$^{-/-}$ and *Pycard*$^{-/-}$ DCs with AlOH tips and observed no defects in binding intensities (**Fig. 5a**).

Alum-trained DCs mediate strong binding to CD4$^+$ T cells

A set of signals that originate from DCs probably mediates alum's adjuvant properties that affect adaptive immune responses *in vivo*. We first tested whether alum-protein aggregates facilitate antigen

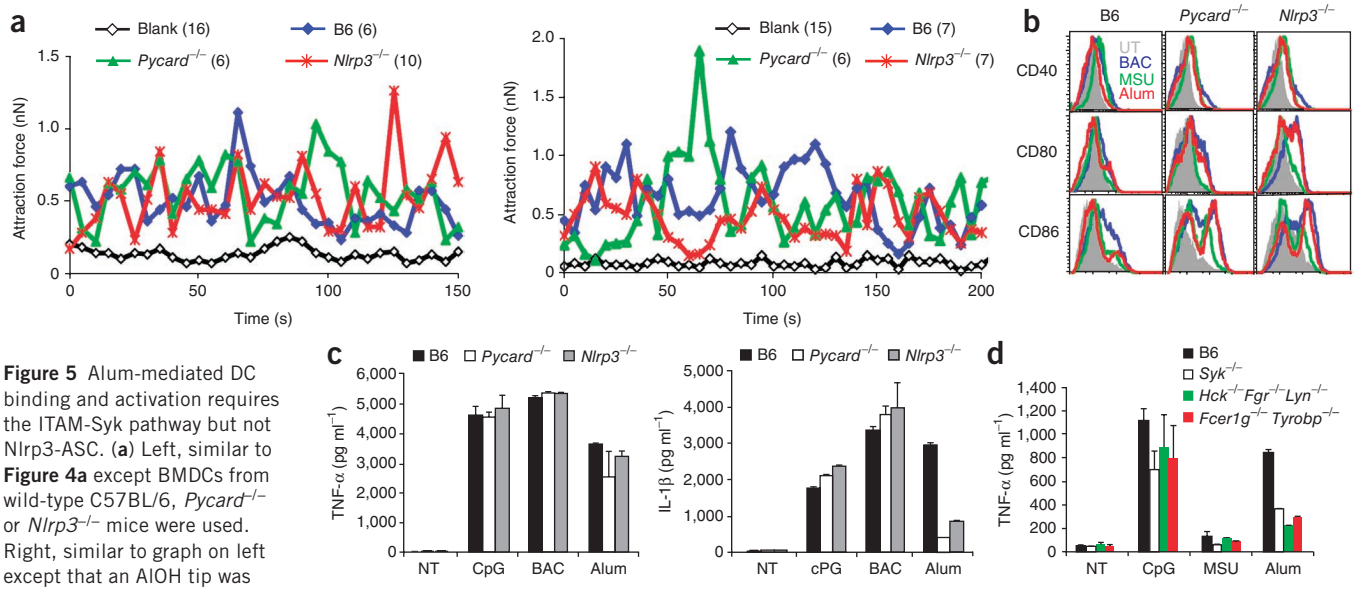

Figure 5 Alum-mediated DC binding and activation requires the ITAM-Syk pathway but not Nlrp3-ASC. (**a**) Left, similar to **Figure 4a** except BMDCs from wild-type C57BL/6, *Pycard*$^{-/-}$ or *Nlrp3*$^{-/-}$ mice were used. Right, similar to graph on left except that an AlOH tip was used. (**b**) FACS analysis of CD40, CD80 and CD86 expression on BMDCs from wild-type, *Nlrp3*$^{-/-}$ and *Pycard*$^{-/-}$ mice left untreated or activated with MSU, bacteria (BAC, killed DH5α *Escherichia coli*) or CsAl precipitate for 24 h. (**c**) ELISA results of TNF-α (left) and IL-1β (right) production from DCs left untreated or activated with CpG, *E. coli* or CsAl precipitate for 6h. The loss of IL-1β production in *Pycard*$^{-/-}$ and *Nlrp3*$^{-/-}$ DCs confirms their deficiencies. (**d**) Similar to **c** except BMDCs from wild-type, Syk-, Src- or ITAM-deficient *Fcer1g*$^{-/-}$ *Tyrobp*$^{-/-}$ DCs were used. MSU, known to trigger very little or no TNF-α production from BMDCs (our own observation), was used as a baseline control.

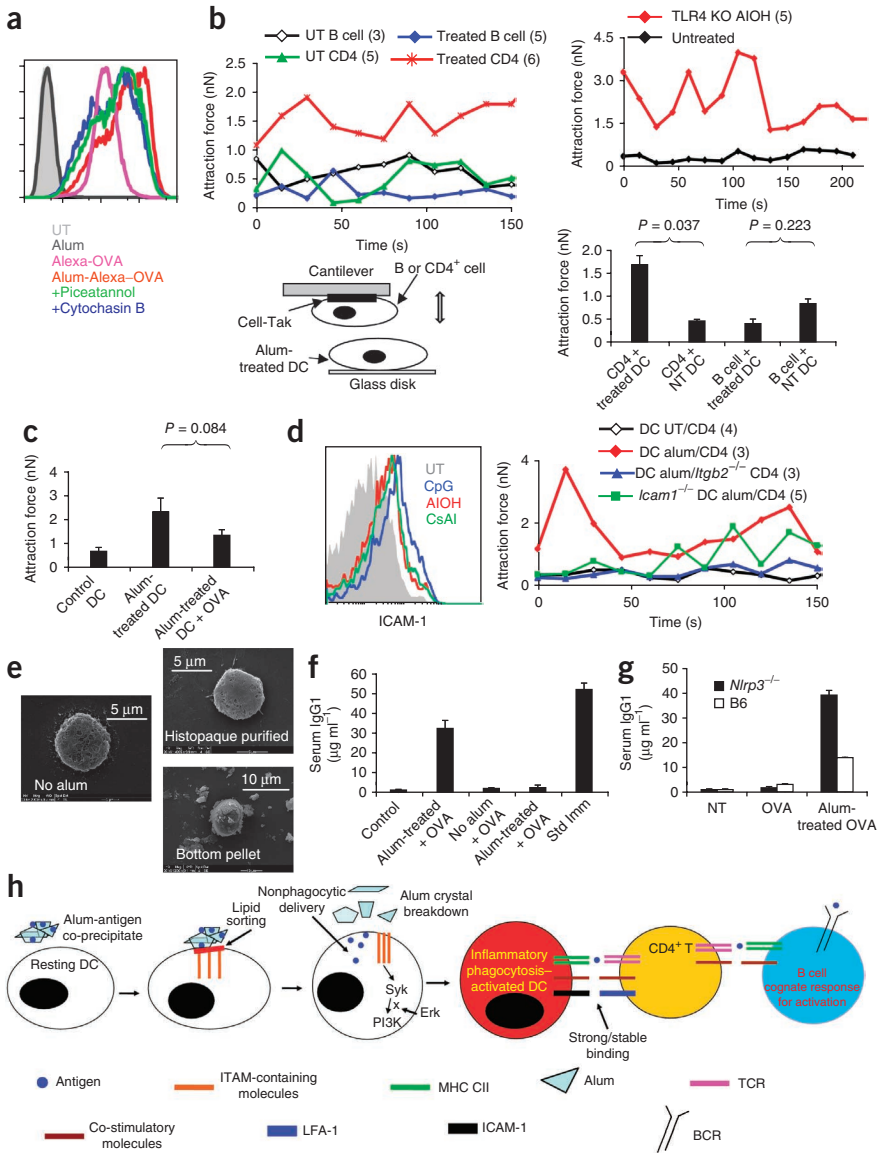

Figure 6 DCs following alum contact gain strong adhesion to CD4 T cells. (**a**) Alexa levels in untreated or BMDCs incubated with CsAl precipitate, Alexa-OVA and conjugated CsAl precipitate–Alexa-OVA as measured by FACS after 2 h. Piceatannol or cytochalasin B was also incubated with CsAl–Alexa-OVA conjugates. (**b**) Top left, splenic B or CD4+ cell binding by DC2.4 cells treated with CsAl precipitate for 4 h. Excess alum was washed away before the binding assay. The top right graph is similar to the left except that BMDCs from TLR4-knockout mice were treated with AlOH. Bottom right, identical data to those at top left depicted in a bar graph for better statistical representation; one-way analysis of variance (ANOVA) for all four is 0.014. (**c**) Similar to **b** bottom right panel except that DCs were pretreated with soluble OVA for 2 h before the reading and that the approaching cell was a magnetic cell sorting–purified splenic OT-II T cell. One-way ANOVA for all four is 0.022. (**d**) Left, BMDC surface expression of ICAM-1 after treatment with AlOH, CsAl or CpG for 24 h was analyzed by FACS with YN1/1.7 antibody. Right, similar to **b** except that untreated, alum-treated wild-type or alum-treated *Icam1*$^{-/-}$ BMDCs were used to make contact with either wild-type CD4+ T cells or LFA-1–knockout CD4+ T cells. (**e**) SEM image of a magnetic cell sorting–purified untreated splenic DC (left) and a DC treated with alum with subsequent Histopaque gradient purification (top right). Bottom right, a DC recovered from the pellet. (**f**) Serum OVA-specific IgG1 titers measured by ELISA 2 weeks after C57BL/6 mice were intravenously immunized with OVA and DC treated with CsAl precipitate and purified with a Histopaque gradient. Standard immunization control is CsAl-based standard OVA immunization. Control is an untreated mouse serum. (**g**) Similar to **e**, except that *Nlrp3*$^{-/-}$ DCs were used. (**h**) A proposed mechanism of how alum invokes the humoral immune response in vaccination. In response to the alum-antigen mixture, DC membrane lipids serve as a surrogate receptor to the crystal surface. The ensuing lipid sorting triggers the aggregation of ITAM containing molecules, Syk recruitment and PI3K activation. However, alum does not enter DCs; it instead delivers the antigen into the DCs via endocytic uptake. DCs process the antigen in their MHC class II compartment and at the same time become activated as a consequence of the inflammatory phagocytosis. The activated DCs strongly engage CD4+ cells via ICAM-1 and LFA-1 binding, leading to the subsequent cognate B cell activation. Here cross-presentation of MHC class I antigens is absent, resulting in no CTL induction.

uptake by DCs. Alexa-OVA–alum conjugates increased uptake of antigen (**Fig. 6a**). Notably, piceatannol (Syk inhibitor) and cytochalasin B (actin inhibitor) had very little effect on fluorescence uptake. In line with the paucity of internalized aluminum in DCs, these results suggest that protein-alum conjugates break down the cell membrane and release antigen into DCs by mechanisms other than phagocytosis. To mediate antibody responses, DCs must present antigen to other cell types, such as B or CD4+ T cells. To examine whether alum stimulated-DCs have enhanced ability to engage these two cell types, we glued a CD4+ T cell or a B cell to an AFM tip and recorded their binding intensities with DCs. DCs treated with CsAl had no enhanced binding to B cells (**Fig. 6b**). In contrast, the same DCs had intense binding to CD4+ T cells (**Fig. 6b**). This result was reproduced with TLR4-deficient BMDCs (**Fig. 6b**). Furthermore, these force interactions were antigen independent and became more consistent over time, devoid of the peaks and valleys (see CD4 control) (**Fig. 6b**). Using OVA antigen and OT-II (OVA-specific) T cells, we next analyzed the effect of alum on DCs in specific antigen presentation. DCs pretreated with alum and soluble OVA did not show an enhanced binding to OT-II T cells compared to OVA-loaded DCs alone (**Fig. 6c**).

To study the nature of this antigen-nonspecific binding, we analyzed the expression of ICAM-1 on DCs. ICAM-1 expression was upregulated by alum (**Fig. 6d**). We repeated the DC T cell assays with LFA-1–knockout T cells and observed no enhanced binding with alum-treated DCs (**Fig. 6d**). Blocking antibodies against α_4 integrin and L-selectin did not reduce the binding (data not shown). Therefore, the main driving force of tighter binding between CD4+ T cells and alum-treated DCs is LFA-1 and ICAM-1 interaction. Alum-treated ICAM-1–knockout

BMDCs were also approached by $CD4^+$ T cells on a tip. Notably, the binding was not completely abolished in some cases (**Fig. 6d**). It is likely that ICAM-1–knockout DCs may have a compensatory suboptimal adhesion mechanism to replace ICAM-1. Taken together, these data show that alum-stimulated DCs efficiently engage $CD4^+$ T cells but not B cells. Furthermore, alum facilitates the initial contact affinity between the two cell types irrespective of antigen recognition.

Alum-trained DCs can transfer alum adjuvanticity

If DCs are the sole conduit of alum's effect, then alum-treated DCs should deliver the adjuvanticity in the absence of alum if antigen is provided otherwise. We treated DCs with CsAl for 2 h. Potentially confounding DCs that contained intracellular or extracellular alum (heavier) were removed using a Histopaque gradient. Alum-treated DCs isolated and purified in this manner showed no detectable alum crystal (**Fig. 6e**). Next, we transferred purified alum-treated DCs to C57BL/6 mice along with OVA. At 2 weeks, we measured OVA-specific antibody titers. DCs pretreated with alum were sufficient to enhance an OVA-specific antibody response, similar to a conventional immunization protocol of subcutaneous injection of CsAl and OVA mixture (**Fig. 6f**). Consistent with the membrane-proximal effects of alum, *Nlrp3*$^{-/-}$ DCs transferred the adjuvanticity similarly to wild-type DCs, suggesting that the Nlrp3 inflammasome is dispensable in the alum-dependent, DC-mediated adjuvant effect (**Fig. 6g**). We believe that, collectively, our work reveals an operational mechanism of alum that pertains to common human vaccination practices (**Fig. 6h**).

DISCUSSION

Our results explain why alum induces primarily an antibody response while sparing cellular immunity. Most particulate antigens are engulfed via phagocytosis. This mode of antigen delivery triggers cross-presentation via one of several proposed phagosome to cytosol/ER antigen transfer mechanisms[34,35]. We discovered that phagocytosis does not come to its completion for alum, and the antigen is delivered in its soluble form. Therefore, the antigen can only enter via another endocytic pathway. Previously, we reported that uric acid was a chief endogenous danger signal mainly for cytolytic T cell (CTL) induction[36,37]. Latex beads and MSU crystals, both efficiently phagocytosed by DCs, trigger cross-presentation and CTL responses[36,38]. This report provides evidence that these solids interact with DCs differently; alum promotes nonphagocytic antigen uptake, which is in line with endosomal processing of CD4-dependent antigens needed to promote humoral immunity. However, it is important to understand the limitations of our work. This report does not directly address why alum causes abortive phagocytosis. Alum's weak crystalline structure may not stand the physical forces deployed during phagocytosis of harder crystals, such as MSU. It may trigger a signaling cascade that does not result in complete phagocytosis. Another note of caution is that such a rapid and abortive phagocytic activity is seen with DCs under our unique experimental settings. This is in contrast with other phagocytes, such as macrophages, which can phagocytose alum particles as measured by more conventional imaging techniques[9,39]. In addition, because there is no ideal way of performing the same assay *in vivo*, our results do not rule out other cell types engaging alum *in vivo*.

The role of Nlrp3-ASC–caspase-1 complex in sensing solid structures (including MSU and alum) has been a topic of discussion in the field, as IL-1β production was lost in mice deficient for these genes[7,30,40]. This finding suggests a sequence in the signaling cascade but does not necessarily infer any sensing mechanisms, especially when these proteins are sequestered by the plasma membrane. Loss of the initial sensor should completely abolish any responses as the result of contact. In this report, we find this part to be played by membrane lipids.

It seems that production of cytokines other than IL-1β and surface co-stimulatory molecule upregulation are not affected by the loss of the inflammasome. This is a subtle, but crucial, issue in the discussion of immunity versus inflammation: the boundary between adjuvanticity and inflammatory responses. It has been pointed out that IL-1β produced by APCs is not for their own consumption but rather to promote systemic inflammation via IL-1 receptor on nonhematopoietic tissues[41]. Presumably, APCs at the stage of IL-1β production have been activated. Our work suggests that Nlrp3 is dispensable for alum's adjuvanticity, despite its capacity to drive systemic inflammation otherwise.

Notably, in our system IL-1β production was intact without alum entering DCs. This implies a signaling mechanism from the cellular membrane to the Nlrp3 inflammasome. One apparent path is via caspase recruitment domain–containing protein -9 (CARD9), as it has been suggested that CARD9 is downstream of Syk activation, and CARD9 activation leads to pro–IL-1β synthesis[42,43]. For the pro–IL-1β to IL-1β conversion, alum provides a contrast to other insoluble crystals. Structurally strong solids are usually phagocytosed, which is an observation that has been taken to suggest that inflammasome activation is always coupled to phagocytic uptake[44]. Our results suggest that membrane lipid sorting by itself may be sufficient to induce pro–IL-1β processing[45].

Our results support previous work demonstrating that DCs, but not macrophages, eosinophils or mast cells, are essential to alum's adjuvanticity[12,46]. The key difference between DCs and macrophages seems to be the hyperactivity of Erk on macrophages, which could downregulate PI3K-required phagocytic signaling. Although DCs are sufficient to transduce alum's adjuvanticity, we believe that $Gr1^+$ cells may serve as another group of immune cells that can also activate B cells[5]. The connection between the two needs further study. It is noteworthy that BMDCs and DC2.4 cells are not analogous to DCs that interact with alum in a vaccination setting, which calls for future confirmation. Nonetheless, the rapid interaction between alum and DCs provides mechanistic insight as to why antigen retention by alum, or the depot effect, is not necessary. Our results disagree with findings that suggest alum mediates its function by inducing uric acid[6]. Alum contact, at the single-cell level and *in vitro*, triggers phagocytosis-linked signaling, resulting in the expression of co-stimulatory molecules and TNF-α. As such, alum-trained DCs can deliver adjuvanticity in the absence of uric acid. In addition, we recently reported that the precipitation of uric acid from its soluble form *in vivo* relies on the presence of uric acid binding IgM antibodies, which drive the initial nucleation process[47]. In our experimental system, these natural IgM antibodies are absent during the direct activation of DCs by alum *in vitro*. We suggest that alum alone is a direct activator of DCs.

Our results suggest that at least at the initial crystal sensing stage, MSU and alum share a common mechanism[45]. We propose the following model: DC membrane lipids serve as a surrogate receptor for these particles. The ensuing lipid sorting triggers conventional phagocytosis-linked signaling. Alum delivers the antigen into the DC via endocytic uptake. DCs process the antigen in their major histocompatibility complex (MHC) class II compartment and at the same time become activated as a consequence of the phagocytic activation via the ITAM-Syk-PI3K chain of events. The activated DCs strongly engage $CD4^+$ T cells for subsequent B cell activation. This may be the main mechanism of alum's adjuvanticity (**Fig. 6h**).

It is unlikely to be coincidental that MSU and alum use lipid sorting to exert their functionalities. The question is whether the solid-surface–lipid interaction is the primary mechanism for the sensing of solid structures by APCs. We hypothesize on theoretical ground that the plasma membrane of DCs is an essential 'receptor' for solids. The unique feature of the DCs is that they can productively translate these lipid alterations into a signaling cascade, using at least Syk and PI3K, probably owing to the lack of interference from ERK. This may not be surprising from an evolutionary perspective. It is likely that events akin to phagocytosis took place before modern phagocytic receptors came into shape. Lower species, limited by genome sizes, could not produce enough receptors to handle all solid structures. The bilayer membrane is a feature of all nucleated life forms. If lipids have affinity for solid structures, it is possible that such interactions have been used for particle uptake. Although in the mammalian immune system specialized receptors are used for phagocytosis, such as FcRs[31], lipid affinity for solid surfaces may have remained operational to this day[48,49].

This report potentially extends knowledge of immune-sensing mechanisms beyond the confines of proteins into the realm of lipids. It bridges several conceptual gaps in understanding of alum's mechanisms and may in the future serve as a basis for the design of safe and effective vaccines. It will probably suggest a research scheme for tissue interactions with all things solid, such as implants and particles, from an angle that has not been explored before.

METHODS

Methods and any associated references are available in the online version of the paper at http://www.nature.com/naturemedicine/.

Note: Supplementary information is available on the Nature Medicine website.

ACKNOWLEDGMENTS

We thank L. Lanier and C. Lowell (University of California–San Francisco) for providing mouse bone marrows; P. Kubes (University of Calgary) for ICAM-1–, LFA-1– and TLR4-knockout mice; K. Rock (University of Massachusetts Medical School), P. Cresswell (Yale University), G. Dranoff (Harvard Medical School) and R. Yates and J. Deans (University of Calgary) for cell lines, L.J. Shen, M. Ho, Y. Yang and P. Santamaria for manuscript review; C. Olson and T. Fung for statistical software and advice; E. Chau for manuscript editing; F. Oskouie for cell culture assistance; and M. Schoel and W.-D. Xiang for SEM and transmission electron microscopy technical assistance. This work was supported by grants from the US National Institutes of Health to Y.S. and equipment donation from JPK instruments to M.W.A.

AUTHOR CONTRIBUTIONS

Y.S. designed experiments with input from M.W.A. and wrote the manuscript with assistance from T.L.F. and D.A.M. T.L.F. performed the experiments unless indicated otherwise below. G.N. performed EDS and SEM assays and developed methods for lipid-crystal binding analysis. A.H. and A.D.M. performed CD4-DC binding analysis and EDS and SEM work and contributed to bilayer lipid synthesis. M.D.D. performed antibody induction and cytokine studies with assistance from Y.F. S.M.W., P.Z. and C.C.L. performed aliphatic chain extension on cholesterol and sphingomyelin. M.E.S. and A.V. performed western blotting. E.P. provided Langmuir trough and technical assistance. J.T. and D.A.M. provided inflammasome-deficient mice and technical assistance and consultation. M.W.A. supervised all aspects of work involving AFM.

COMPETING FINANCIAL INTERESTS

The authors declare no competing financial interests.

Published online at http://www.nature.com/naturemedicine/.
Reprints and permissions information is available online at http://npg.nature.com/reprintsandpermissions/.

1. Glenny, A.T., Pope, C.G., Waddington, H. & Wallace, V. The antigenic value of toxoid precipitated by potassium alum. Receptors control activation of adaptive immune responses. *J. Pathol. Bacteriol.* **29**, 38–45 (1926).
2. Parham, P. *The Immune System* 2nd ed. Ch. 12 (Garland Science, 2004).
3. Marrack, P., McKee, A.S. & Munks, M.W. Towards an understanding of the adjuvant action of aluminium. *Nat. Rev. Immunol.* **9**, 287–293 (2009).
4. Glenny, A.T., Buttle, G.A.H. & Stevens, M.F. Rate of disappearance of diphtheria toxoid injected into rabbits and guinea-pigs: toxoid precipitated with alum. *J. Pathol. Bacteriol.* **34**, 267–275 (1931).
5. Jordan, M.B., Mills, D.M., Kappler, J., Marrack, P. & Cambier, J.C. Promotion of B cell immune responses via an alum-induced myeloid cell population. *Science* **304**, 1808–1810 (2004).
6. Kool, M. *et al.* Alum adjuvant boosts adaptive immunity by inducing uric acid and activating inflammatory dendritic cells. *J. Exp. Med.* **205**, 869–882 (2008).
7. Eisenbarth, S.C., Colegio, O.R., O'Connor, W., Sutterwala, F.S. & Flavell, R.A. Crucial role for the Nalp3 inflammasome in the immunostimulatory properties of aluminium adjuvants. *Nature* **453**, 1122–1126 (2008).
8. Sharp, F.A. *et al.* Uptake of particulate vaccine adjuvants by dendritic cells activates the NALP3 inflammasome. *Proc. Natl. Acad. Sci. USA* **106**, 870–875 (2009).
9. Hornung, V. *et al.* Silica crystals and aluminum salts activate the NALP3 inflammasome through phagosomal destabilization. *Nat. Immunol.* **9**, 847–856 (2008).
10. Franchi, L. & Nunez, G. The Nlrp3 inflammasome is critical for aluminium hydroxide-mediated IL-1β secretion but dispensable for adjuvant activity. *Eur. J. Immunol.* **38**, 2085–2089 (2008).
11. Kool, M. *et al.* Cutting edge: alum adjuvant stimulates inflammatory dendritic cells through activation of the NALP3 inflammasome. *J. Immunol.* **181**, 3755–3759 (2008).
12. McKee, A.S. *et al.* Alum induces innate immune responses through macrophage and mast cell sensors, but these sensors are not required for alum to act as an adjuvant for specific immunity. *J. Immunol.* **183**, 4403–4414 (2009).
13. Leonenko, Z., Finot, E. & Amrein, M. Adhesive interaction measured between AFM probe and lung epithelial type II cells. *Ultramicroscopy* **107**, 948–953 (2007).
14. Ng, G. *et al.* Receptor-independent, direct membrane binding leads to cell-surface lipid sorting and Syk kinase activation in dendritic cells. *Immunity* **29**, 807–818 (2008).
15. Harlow, E. & Lane, D. *Antibodies—a Laboratory Manual* Ch. 5 (Cold Spring Harbor Laboratory Press, Cold Spring Harbor, New York, 1988).
16. Coligan, J.E. *Short Protocols in Immunology* Ch. 1 (Wiley, 2005).
17. Goldstein, J. *et al. Scanning Electron Microscopy and X-ray Microanalysis* Ch. 7 (Springer, 2003).
18. Garry, V.F., Good, P.F., Manivel, J.C. & Perl, D.P. Investigation of a fatality from nonoccupational aluminum phosphide exposure: measurement of aluminum in tissue and body fluids as a marker of exposure. *J. Lab. Clin. Med.* **122**, 739–747 (1993).
19. Lanier, L.L., Corliss, B.C., Wu, J., Leong, C. & Phillips, J.H. Immunoreceptor DAP12 bearing a tyrosine-based activation motif is involved in activating NK cells. *Nature* **391**, 703–707 (1998).
20. Crowley, M.T. *et al.* A critical role for Syk in signal transduction and phagocytosis mediated by Fcγ receptors on macrophages. *J. Exp. Med.* **186**, 1027–1039 (1997).
21. Fitzer-Attas, C.J. *et al.* Fcγ receptor–mediated phagocytosis in macrophages lacking the Src family tyrosine kinases Hck, Fgr and Lyn. *J. Exp. Med.* **191**, 669–682 (2000).
22. Jiang, K. *et al.* Syk regulation of phosphoinositide 3-kinase–dependent NK cell function. *J. Immunol.* **168**, 3155–3164 (2002).
23. Dai, R., Chen, R. & Li, H. Cross-talk between PI3K/Akt and MEK/ERK pathways mediates endoplasmic reticulum stress-induced cell cycle progression and cell death in human hepatocellular carcinoma cells. *Int. J. Oncol.* **34**, 1749–1757 (2009).
24. Rommel, C. *et al.* Differentiation stage-specific inhibition of the Raf-MEK-ERK pathway by Akt. *Science* **286**, 1738–1741 (1999).
25. Shiratsuchi, H. & Basson, M.D. Extracellular pressure stimulates macrophage phagocytosis by inhibiting a pathway involving FAK and ERK. *Am. J. Physiol. Cell Physiol.* **286**, C1358–C1366 (2004).
26. Kovjazin, R. *et al.* Ferrocene-induced lymphocyte activation and anti-tumor activity is mediated by redox-sensitive signaling. *FASEB J.* **17**, 467–469 (2003).
27. Mathur, R.K., Awasthi, A., Wadhone, P., Ramanamurthy, B. & Saha, B. Reciprocal CD40 signals through p38MAPK and ERK-1/2 induce counteracting immune responses. *Nat. Med.* **10**, 540–544 (2004).
28. Newton, R. *et al.* The MAP kinase inhibitors, PD098059, UO126 and SB203580, inhibit IL-1β–dependent PGE_2 release via mechanistically distinct processes. *Br. J. Pharmacol.* **130**, 1353–1361 (2000).
29. Martinon, F., Mayor, A. & Tschopp, J. The inflammasomes: guardians of the body. *Annu. Rev. Immunol.* **27**, 229–265 (2009).
30. Martinon, F., Petrilli, V., Mayor, A., Tardivel, A. & Tschopp, J. Gout-associated uric acid crystals activate the NALP3 inflammasome. *Nature* **440**, 237–241 (2006).
31. Greenberg, S. & Grinstein, S. Phagocytosis and innate immunity. *Curr. Opin. Immunol.* **14**, 136–145 (2002).
32. Yeung, T. *et al.* Receptor activation alters inner surface potential during phagocytosis. *Science* **313**, 347–351 (2006).
33. Sun, H., Pollock, K.G. & Brewer, J.M. Analysis of the role of vaccine adjuvants in modulating dendritic cell activation and antigen presentation *in vitro*. *Vaccine* **21**, 849–855 (2003).
34. Rock, K.L. & Shen, L. Cross-presentation: underlying mechanisms and role in immune surveillance. *Immunol. Rev.* **207**, 166–183 (2005).
35. Rock, K.L. Exiting the outside world for cross-presentation. *Immunity* **25**, 523–525 (2006).

36. Shi, Y., Evans, J.E. & Rock, K.L. Molecular identification of a danger signal that alerts the immune system to dying cells. *Nature* **425**, 516–521 (2003).
37. Shi, Y., Galusha, S.A. & Rock, K.L. Cutting edge: elimination of an endogenous adjuvant reduces the activation of CD8 T lymphocytes to transplanted cells and in an autoimmune diabetes model. *J. Immunol.* **176**, 3905–3908 (2006).
38. Kovacsovics-Bankowski, M. & Rock, K.L. A phagosome-to-cytosol pathway for exogenous antigens presented on MHC class I molecules. *Science* **267**, 243–246 (1995).
39. Rimaniol, A.C. *et al.* Aluminum hydroxide adjuvant induces macrophage differentiation towards a specialized antigen-presenting cell type. *Vaccine* **22**, 3127–3135 (2004).
40. Martinon, F. Detection of immune danger signals by NALP3. *J. Leukoc. Biol.* **83**, 507–511 (2008).
41. Chen, C.J. *et al.* MyD88-dependent IL-1 receptor signaling is essential for gouty inflammation stimulated by monosodium urate crystals. *J. Clin. Invest.* **116**, 2262–2271 (2006).
42. Gross, O. *et al.* Syk kinase signalling couples to the Nlrp3 inflammasome for anti-fungal host defence. *Nature* **459**, 433–436 (2009).
43. Ruland, J. CARD9 signaling in the innate immune response. *Ann. NY Acad. Sci.* **1143**, 35–44 (2008).
44. Shio, M.T. *et al.* Malarial hemozoin activates the NLRP3 inflammasome through Lyn and Syk kinases. *PLoS Pathog.* **5**, e1000559 (2009).
45. Shi, Y., Mucsi, A.D. & Ng, G. Monosodium urate crystals in inflammation and immunity. *Immunol. Rev.* **233**, 203–217 (2010).
46. De Gregorio, E., D'Oro, U. & Wack, A. Immunology of TLR-independent vaccine adjuvants. *Curr. Opin. Immunol.* **21**, 339–345 (2009).
47. Kanevets, U., Sharma, K., Dresser, K. & Shi, Y. A role of IgM antibodies in monosodium urate crystal formation and associated adjuvanticity. *J. Immunol.* **182**, 1912–1918 (2009).
48. Richter, R., Mukhopadhyay, A. & Brisson, A. Pathways of lipid vesicle deposition on solid surfaces: a combined QCM-D and AFM study. *Biophys. J.* **85**, 3035–3047 (2003).
49. Nollert, P., Kiefer, H. & Jahnig, F. Lipid vesicle adsorption versus formation of planar bilayers on solid surfaces. *Biophys. J.* **69**, 1447–1455 (1995).

ONLINE METHODS

Mice, cells and reagents. C57BL/6, OT-II, *Pycard*$^{-/-}$, *Nlrp3*$^{-/-}$, *Itgb2*$^{-/-}$ (LFA-1 knockout), *Icam1*$^{-/-}$ and *Tlr4*$^{-/-}$ male and female mice were housed at the University of Calgary Animal Research Centre. All mouse experiments were approved by the Animal Protocol Committee of University of Calgary**.** Bone marrow DCs from *Fcer1g*$^{-/-}$ *Tyrobp*$^{-/-}$ (ITAM knockout), Hck$^{-/-}$/Fgr$^{-/-}$/Lyn$^{-/-}$ (Src knockout) and Syk$^{-/-}$ C57BL/6 fetal liver chimera mice were produced from bones as gifts from C. Lowell and L. Lanier. Wild-type C57BL/6 mice were used for all experiments unless indicated otherwise. B cell lines A20, Bjab, Ramos and Raji and macrophage lines J744 and ANA-RY1 were gifts from J. Deans and R. Yates. THP-1 cells (PMA induced) were a gift from P. Cresswell. RAW 264.7 and DC2.4 cells were gifts from K. Rock. FMS-like tyrosine kinase-3 ligand–transfected B16 cells were a gift from G. Dranoff. Flow cytometric analysis and most reagents used in this work have been described previously[14,50]. All antibodies and ELISA kits were from eBioscience. OVA, cytochalasin B, MBCD, piceatannol, PMA and Histopaque 1119 were purchased from Sigma. UO126, PD 098059 and ferrocene were from Tocris. Wortmannin was from A.G. Scientific. All lipid probes were purchased from Molecular Probes (Invitrogen) or Avanti Lipids. Cell Tak was from BD. Cesium alum (CsAl, aluminum cesium sulfate dodecahydrate) and Imject were from Sigma and Fisher, respectively. Alexa 488-OVA was from Invitrogen. MACS beads were from Miltenyi. Complete Freund's adjuvant was from Rockland.

Bone marrow DCs were grown with IL-4 and GM-CSF[14]. On the sixth day of DC growth, cells were gently washed once with PBS and replaced with fresh cell culture medium (RPMI 1640 with 10% FBS). DCs were treated with the following reagents: CpG (5 μg ml^{-1}), bacteria (0.25 μg ml^{-1}, killed *E. coli*)[50], CsAl precipitate (5mg ml^{-1}) or MSU (200 μg ml^{-1}) and incubated at 37 °C, 5% CO_2. Supernatant was collected at 6 and 24 h and analyzed with Ready-Set-Go ELISA kits. At 24 h, cells were scraped from the wells and stained for CD11c in addition to CD86, CD80 and CD40 and analyzed by FACS (BD). For AFM analysis, cells were grown on glass disks. B cells that are nonadherent to glass were stabilized by precoating with poly-D-lysine per manufacturer's instructions (BD). Glass cover slides were soaked with 25 μg ml^{-1} poly-D-lysine in 1.25 ml PBS per well for 45 min, with agitation every 15 min. Cover slides were then dried and submerged in culture medium over night. Glass disks (VWR) used for AFM had a 22-mm diameter and were washed with ethanol and distilled water before being plated with cells inside six-well plates. Cells were cultured at 1 / 32 normal culture density.

Additional methods. Detailed methodology is described in the **Supplementary Methods**.

50. Desrosiers, M.D. *et al.* Adenosine deamination sustains dendritic cell activation in inflammation. *J. Immunol.* **179**, 1884–1892 (2007).

doi:10.1038/nm.2306